Received: 30 August 2019 | Revised: 8 June 2020 | Accepted: 12 June 2020

DOI: 10.1002/jbm.a.37052

ORIGINAL ARTICLE

Society For Biomaterials | WILEY

Influence of nano-hydroxyapatite coating implants on gene expression of osteogenic markers and micro-CT parameters. An in vivo study in diabetic rats

Paula Gabriela Faciola Pessôa de Oliveira[1] | Mariana Sales de Melo Soares[1] | Adriana Maria Mariano Silveira e Souza[1] | Mário Taba Jr[1] | Daniela Bazan Palioto[1] | Michel Reis Messora[1] | Bruna Ghiraldini[2] | Felipe Anderson de Sousa Nunes[1] | Sérgio Luís Scombatti de Souza[1]

[1]Department of Oral and Maxillofacial Surgery and Periodontology, FORP/USP, University of São Paulo, Ribeirão Preto, São Paulo, Brazil

[2]Paulista University, School of Dentistry, São Paulo, São Paulo, Brazil

Correspondence
Sérgio Luís Scombatti de Souza Departament of Oral & Maxillofacial Surgery and Periodontology School of Dentistry of Ribeirão Preto University of São Paulo Av do Café, s/n. 14040-904 Ribeirão Preto, SP, Brazil.
Email: scombatti@forp.usp.br

Funding information
National Council of Scientific and Technological Development (CNPq, Brazil), Grant/Award Number: Grant number: 446840/2014-9; State of Sao Paulo Research Foundation (FAPESP, Brazil), Grant/Award Numbers: 2015/09879-0, 2016/14584-2

Abstract

This study evaluated the response of a nano-hydroxyapatite coating implant through gene expression analysis (runt-related transcription factor 2 (Runx2), alkaline phosphatase (Alp), osteopontin (Opn), osteocalcin (Oc), receptor activator of nuclear factor-kappa B (Rank), receptor activator of nuclear factor-kappa B ligand (Rank-L), and osteoprotegerin (Opg)). Three-dimensional evaluation (percent bone volume (BV/TV); percent intersection surface (BIC); bone surface/volume ratio (BS/BV); and total porosity (To.Po)) were also analyzed. Mini implants were surgically placed in tibias of both healthy and diabetic rats. The animals were euthanized at 7 and 30 days. Evaluating all factors the relative expression of Rank showed that NANO surface presented the best results at 7 days (diabetic rats). Furthermore the levels of Runx2, Alp, Oc, and Opn suggest an increase in osteoblasts proliferation, especially in early stages of osseointegration. %BIC in healthy and diabetic (7 days) depicted statistically significant differences for NANO group. BV/TV, BS/BV and To.Po demonstrated higher values for NANO group in all evaluated time point and irrespective of systemic condition, but BS/BV 30 days (healthy rat) and 7 and 30 days (diabetic rat). Microtomographic and gene expression analyses have shown the benefits of nano-hydroxyapatite coated implants in promoting new bone formation in diabetic rats.

KEYWORDS

dental implants, diabetes mellitus, gene expression, microtomography, osseointegration

1 | INTRODUCTION

Osseointegration is a very close contact that is established between bone and implants observed at the optical microscopy level. This event allows implants to replace load-bearing organs, restoring their form and function (Albrektsson, Branemark, Hansson, & Lindstrom, 1981). Implant dentistry has been considered a predictable treatment, with higher rates of success (greater than 90%) (Chuang, Tian, Wei, & Dodson, 2001).

Diabetes mellitus (DM) is a metabolic disease caused by hyperglycemia due to secretion or abnormal response of cells to insulin, which is a hormone, produced by beta cells in the pancreatic islets of Langerhans (Expert Committee on the Diagnosis and Classification of Diabetes Mellitus, 2003). Type 1 diabetes is associated to pancreatic

The authors have complete independence in the results and did not receive any kind of aid.

β-cell destruction, and requires insulin therapy, while Type 2 diabetes is characterized by a relative rather than total insulin deficiency, and is usually a multifactorial disorder (Retzepi & Donos, 2010). The pathognomonic characteristic of DM, chronic hyperglycemia, causes severe damage to bone biology. Nonetheless, patients with controlled diabetes are candidates for treatment with dental implants with increasing success (Courtney Jr., Snider, & Cottrell, 2010). However, for those with uncontrolled levels, this treatment is a contra-indication.

Studies have shown that modifications in implant topography, energy, wettability, chemistry or an association of them affect cell proliferation, differentiation, adhesion, migration, messenger ribonucleic acid (mRNA) expression, protein synthesis and secretion, which may have a beneficial effect on bone formation (Jimbo et al., 2011; Souza et al., 2018). It was reported that increasing the implant surface texture by a variety of processes, such as acid etching and grit-blasting, positively affected early healing, leading to greater degrees of integration and biomechanical fixation (Coelho et al., 2009). Beyond the texture modifications, chemical changes, such as the incorporation of hydroxyapatite (HA) as a surface coating, resulted in highly osseoconductive surfaces (Coelho et al., 2009).

Nano-scale roughness may play an important role for bone biology, due to the size of proteins and cell membrane receptors corresponds to surface topography on this length scale. Gittens and collaborators reported that nano-scale changes markedly enhanced the differentiation of pre-osteoblasts, which showed significantly higher levels of osteocalcin and osteoprotegerin expression in vitro (Gittens et al., 2011). Furthermore, Meirelles and collaborators performed an animal study with implants containing nanostructures and polished implants, and observed that the former had higher bone-to-implant contact than the latter implant surfaces (Meirelles, Arvidsson, Albrektsson, & Wennerberg, 2007). These descriptions indicate that osteoblasts respond to topographical alterations at the nanometer scale. Additionally, reduced osteoid formation, delayed osteoid mineralization, and reduced overall bone volume and maturation in hyperglycemia were observed by Goodman & Hori, (1984).

Micro-computed tomography (micro-CT) is a powerful device in dental research and with potential for qualitative and quantitative analyses of implant osseointegration (Li et al., 2015; Vandeweghe, Coelho, Vanhove, Wennerberg, & Jimbo, 2013). It is extensively used for observing and analyzing the internal structure of hard tissue due to its advantages of rapidity, reproducibility, and nondestructiveness (Feldkamp, Goldstein, Parfitt, Jesion, & Kleerekoper, 1989). Additionally, micro-CT also allows for accurate three-dimensional (3D) measurements of bone-to-implant contact (BIC), and is used to measure several variables, such as bone volume (BV), total volume (TV), bone volume fraction (BV/TV), trabecular thickness (Tb.Th), trabecular number (Tb.N), and trabecular separation (Tb.Sp) (Odgaard, 1997).

Ajami et al. (2014) performed a microtomographic and histologic study using euglycemic and hyperglycemic rats, and concluded that deficient implant integration in hyperglycemia is cancelled by the addition of nanotopographical properties to an underlying microtopographically complex implant surface. Thus, the purpose of this study was to evaluate, in healthy and diabetic rats, the response of a new topography implant surface (nano-hydroxyapatite coating) through gene expression analysis (evaluating Runx2, Alp, Opn, Oc, Rank, Rank-L, and Opg) and a 3D evaluation using micro-CT (evaluating the percent bone volume (BV/TV, %); percent intersection surface (BIC, %); bone surface/volume ratio (BS/BV, mm); and total porosity (To.Po, %)), with the aim to investigate the surface modifications at the nano-scale in a compromise model of bone healing at two different time points (7 and 30 days).

2 | MATERIALS AND METHODS

2.1 | Implant surfaces

The dimension of all the implants was 1.4 mm in diameter and 2.7 mm in length (SIN implantes, São Paulo, São Paulo, Brazil). This study analyzed commercially pure titanium implants (Grade 4). Three different surfaces were evaluated: machined, double acid etched (DAE) and nano-hydroxyapatite coating applied on DAE surface (NANO).

2.1.1 | Machined surface

The machined implants did not receive any surface treatment. They were produced according to the project characteristics of diameter and length, in CNC lathe machines, from commercially pure titanium (Grade 4) cylindrical bars. During the machining process, the implants are inspected for their critical dimensional characteristics, shape/position, surface finish and mechanical requirements. After that, they received automated pre-washing by Centrifugal Disc units, and hygiene process, carried out inside controlled rooms (Clean Room), in high performance automated cleaning systems (Ultrasonic Cleaning Systems). Then, they were packed by an automated process and sterilized for use in the study.

Although machined implants are rarely used today, modern implant surfaces are often compared with them. In the present study, machined implants were considered the negative control group.

2.1.2 | DAE surface

The DAE surface was obtained from a machined implant surface that received baths of nitric acid followed by sulfuric acid, in a micro corrosion process. In the present study, DAE surface was considered a positive control group.

2.1.3 | NANO surface

For the NANO surface treatment, a DAE implant surface was processed according to (Kjellin & Andersson, 2012). Briefly, coating liquid containing nanohydroxyapatite crystals was applied on top of the implant to be coated, and the implant was placed on a spin coater

device. The implant was rotated at 2600 rpm for 3 s, for homogenization of the liquid over the entire surface, and allowed to dry at 10 min in room temperature. The implant was then placed in an oven at 450°C for 5 min, for sintering and stable adhesion of the HA crystals.

2.2 | Implant surface characterization

To identify and characterize the elemental composition and chemical interactions present on implants surface, X-ray photoelectron spectroscopy (XPS) measurements were performed using a PHI 5000C ESCA System; (PerkinElmer Inc.,Waltham, MA). Spectra were obtained at an operating angle of 45°, at 200 W with an Al K-alpha excitation source (Figure 1). A Leo Ultra 55 FEG scanning electron microscope (SEM) (Zeiss, Oberkochen, Germany) was used to analyze the surfaces. The ultrastructural morphology of these surfaces is represented in Figure 2 by scanning electron micrographs.

2.3 | Animals

This research was authorized by Animal Experimentation Ethics Committee at the FORP/USP (protocol 2014.1.1083.58.4; November 2014).

Seventy-two adult male Wistar rats (250–300 g) were selected for the study. The rats had free access to water and a standard diet, and were kept in plastic cages. Previous to the surgical procedures, the animals were allowed to acclimatize to the laboratory environment for 7 days. The animals were randomly allocated to the diabetes mellitus group or control group.

2.4 | Induction of DM

Diabetes was induced by a single intraperitoneal injection (i.p.) of Streptozotocin (STZ, 60 mg/kg, Sigma, St. Louis, Missouri), dissolved in 0.2 ml citrate buffered solution (0.01 M, pH 4.5) (n = 36). In the healthy group, an i.p. injection of the vehicle (1 ml/kg) (n = 36) was applied. Blood glucose levels were dosed at the day of implantation and before euthanasia through a superficial puncture in the distal tail, and instantly measured with a glucometer (Accu-Check Active monitoring system, Roche Diagnostics, Rotkreuz, Zug, Switzerland). Only rats with glucose levels higher than 300 mg/dl were considered diabetic and included in the study (Margonar et al., 2003).

2.5 | Surgical procedures

General anesthesia was performed by an injection of 100–130 μl/(100 g animal weight) in a 4:3 combination of ketamine (74.1 mg/g of 10% ketamine hydrochloride; Agener, União Química Farmacêutica Nacional S/A, Embu-Guaçu, São Paulo, Brazil) and xylazine (11.2 mg/kg dopaser; Calier Laboratories S/A, Catalonia, Barcelona, Spain). Next, trichotomy and antisepsis with iodine solution 10% (Rioquímica Ind. Farmacêutica, São José do Rio Preto, São Paulo, Brazil) at the medial side of the right and left tibia were performed.

Using a type 15C scalpel blade (Swann-Morton, Sheffield, England), a 15-mm incision was done on the medial side of both tibias. After dissection with a periosteum separator, bone was exposed, washed with abundant sterile saline solution (0.9%) and drilled with a 2.0 mm length pilot drill (SIN implantes, São Paulo, São Paulo, Brazil) using an electric implant motor (Dentscler, Ribeirão Preto, São Paulo, Brazil) at 1000 rotation per minute (rpm). The perforation was made under uninterrupted irrigation with sterile saline solution (0.9%). A custom-made titanium implant (SIN implantes, São Paulo, São Paulo, Brazil) was randomly installed in the left or right tibia using a hand driver key (SIN implantes, São Paulo, São Paulo, Brazil). Incisions were sutured with 5–0 coated Vicryl suture (Vicryl Ethicon 5.0, Johnson Prod., São José dos Campos, São Paulo, Brasil).

After the surgical procedure, the animals were observed daily for symptoms of pain, dehiscence, infection, limited movement, lack of appetite or weight loss. To avoid pain after surgery, a single dose of anti-inflammatory (ketoprofen 0,05 mg/kg), and antibiotic (penicillin 24.000 IU/kg) were also administered. All rats had a good postoperative and did not need supplementary doses of prescriptions.

2.6 | Experimental groups

The 62 animals were indiscriminately separated into six experimental groups containing 12 animals each, and the groups were classified

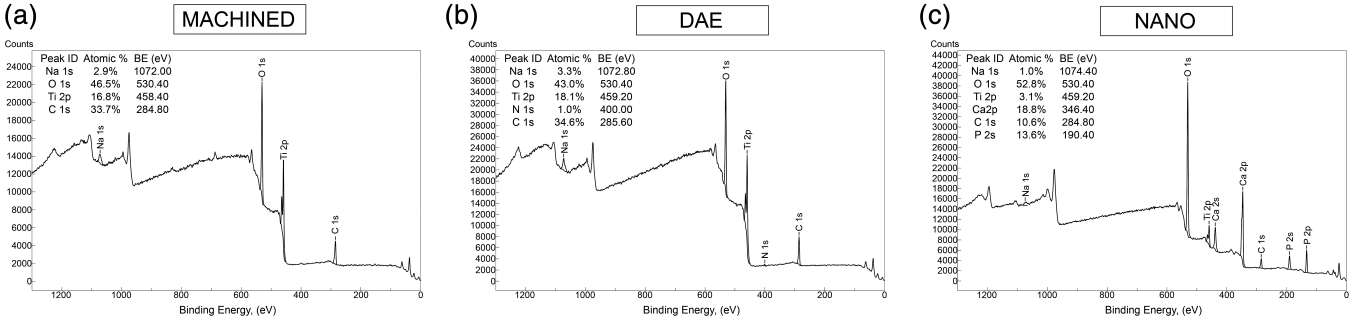

FIGURE 1 XPS spectra from machined (a), DAE (b) and NANO HA (c) surfaces

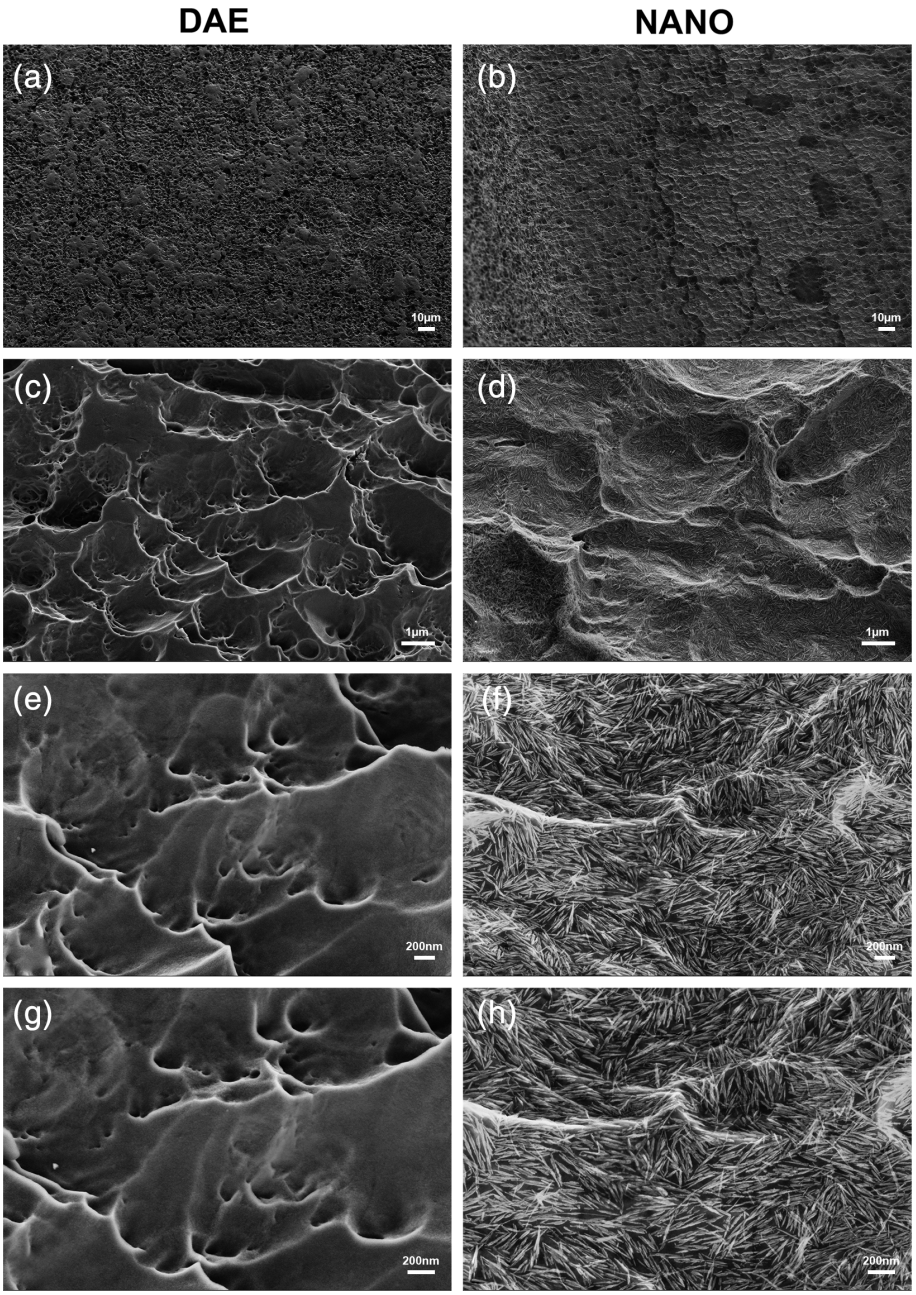

FIGURE 2 (a–h) High-resolution scanning electron micrographs of titanium surfaces. DAE (a/c/e/g) and NANO HA surfaces (b/d/e/h) with magnification of 1.00x (a/b), 20.000x (c/d) 60.000x (e/f) and 80.000x (g/h). NANO HA exhibits a network of nanopores, and the addition of nanoparticles did not alter the microtopography, but increased the contact surface on nanometric scale

according to the implants surface treatments and the presence or absence of diabetes in rats: G1, machined mini implants installed in healthy animals; G2, double acid etched (DAE) mini implants installed in healthy animals; G3, nano-hydroxyapatite (NANO) covered mini implants installed in healthy animals; G4, machined mini implants installed in diabetic animals; G5, DAE mini implants installed in diabetic rats; and G6, NANO covered mini implants installed in diabetic animals.

The rats were euthanized 7 and 30 days after implants placement (36 animals in each period, 18 healthy and 18 diabetic, 6 from each group) by the intraperitoneal injection of a deadly dose (150 mg/kg) of sodium thiopental (Thiopentax, Cristália, São Paulo, Brazil). The implant and surrounding bone from right tibia were collected with the use of a Φ3.0 mm trephine bur (Alpha instruments, Ribeirão Preto, São Paulo, Brazil); thereafter, the bone tissue was frozen at −80°C until analysis. The left tibia was removed and fixed in 10% neutral formalin for 48 hr for micro-CT analysis. Gene expression of Runx2, Alp, Opn, Oc, Rank, Rankl and Opg, and micro-CT parameters of percent bone volume (BV/TV, %), percent intersection surface (BIC, %), bone surface/volume ratio (BS/BV, mm), and total porosity (To.Po, %), were evaluated.

2.7 | Quantitative real-time polymerase chain reaction assay

Quantitative real-time polymerase chain reaction (qRT-PCR) was executed at 7 and 30 days to analyze the gene expression of Runx2, Alp,

Oc, Op, Rank, RankL and Opg. The implants were removed and bone fragments of two specimens of the same group were put together and allowed to macerate, and the total RNA was extracted with Trizol reagent (Life Technologies – Invitrogen, Carlsbad, CA) followed by SV Total RNA Isolation System (Promega, Madison, Wisconsin) following the manufacturer's instructions. The concentration and purity were decided using a NanoVue spectrophotometer (GE Healthcare, Little Chalfont, Buckinghamshire, United Kingdom) by optical density at a wavelength of 260 and 260:280 nm, respectively, and only samples presenting 260:280 ratios higher than 1.8 were analyzed. The integrity of ribosomal RNA was evaluated using the 2100 Bioanalyzer (Agilent Technologies, Stockport, Manchester, United Kingdom). Samples with RNA Integrity Number (RIN) values equal or higher than 7 were used to synthesize complementary DNA (cDNA) from 1 μg of total RNA, using cDNA High-Capacity cDNA Reverse Transcription Kit (Applied Biosystems, Foster City, California), following to manufacturer's instructions. Real-time PCR was done in triplicate and executed in a StepOnePlus Real-Time PCR System (Thermo Fisher Scientific, Waltham, Massachusetts); the thermal cycling specifications were 50°C (2 min), 95°C (20 s), and 40 cycles of 95°C (3 s) and 60°C (30 s) in a 10 μl reaction volume, using 5 μl of TaqMan universal PCR master mix AmpErase UNG 2X (Life Technologies-Invitrogen), 0.5 μl of TaqMan probes (20X TaqMan gene expression assay mix) and 1.125 μg/μl of cDNA. The relative gene expression was measured in reference to glyceraldehyde-3-phosphate dehydrogenase (GAPDH) expression and the real variations were expressed relative to the gene expression of the healthy machined 7 days group, using the comparative delta-Ct method (Livak & Schmittgen, 2001).

2.8 | Computed microtomographic analysis

The samples were fixed in 10% buffered formalin solution (pH = 7) during 2 days. Sequentially, the micro-CT analysis was carried out with the aid of a Skyscan 1,172 micro-CT scanner (Bruker, Kontich, Antwerp, Belgium). All scans were obtained at 100 kV and 100 A, with an aluminum–copper filter to improve the contrast, and set at 5.87 mm pixel size, 360 rotation, 4 frames averaging, a rotation step of 0.40. The reconstruction software (NRecon v.1.6.10.4, Bruker, Kontich, Antwerp, Belgium) was used to create the images, which were positioned according to the implant long axis.

The 3D analysis was done using the CTAn software (CTAn., v. 1.15.4.0, Bruker, Kontich, Antwerp, Belgium) and the following parameters were analyzed: percent bone volume (BV/TV, %), percent intersection surface (BIC, %), bone surface/volume ratio (BS/BV, mm), and total porosity (To.Po, %).

A task list was created (custom processing) to automatically obtain the values of the selected parameters for inter-group comparisons. The measurements were performed 1 mm from the top of the implant, reaching its entire length. This process involved the determination of the region of interest (ROI). The collective value of all ROIs over a contiguous set of cross-sectional image slices was used to define the volume of interest (VOI), representing the selected 3D volume. The binarization was done using the gray scale defined by a density of 35–150 for bone, and 150–255 for implant. All micro-CT analyzes were done by a single researcher who was unaware of the identities of the different experimental groups.

2.9 | Statistical analysis

All variables are shown as a function of mean values with the corresponding 95% confidence interval (mean ± 95% CI). Previous analyses have shown undistinguishable variances (Levene test, all $p > .25$). Additionally, data were collected and aligned along a linear mixed model with fixed factors of time (7 and 30 days), systemic condition (healthy and diabetic) and surface chemistry/texture modifications (machined, DAE and NANO HA) at a random intercept. After administering a significant omnibus test, post-hoc comparison of the experimental groups means was accumulated using Tukey test. The analysis was accomplished using SPSS (IBM SPSS 23, IBM Corp., Armonk, NY).

3 | RESULTS

No postoperative infections and/or other immediate clinical concerns accompanied the surgical procedures or follow-up. All animals regained consciousness after 30 min post-surgery and post-operative healing was uneventful. No surgical complications were observed and surgical wound healing was considered satisfactory for all study animals.

Figure 3 shows the blood glucose (mg/dl) of healthy and diabetic groups at surgery day and before euthanasia. The values for the healthy (surgery: 89.55 ± 8.88 and euthanasia: 92.19 ± 9.67) and diabetic (surgery: 499.88 ± 62.27 and euthanasia: 544.63 ± 57.07) rat confirm the establishment of the diabetic model.

Figures 4 and 5 showed the relative gene expression of osteogenic markers, including Runx2 (4A), Alp (4B), Opn (4C), Oc (4D), Rank (5A), RankL (5B) and Opg (5C), detected by qRT-PCR after 7 and

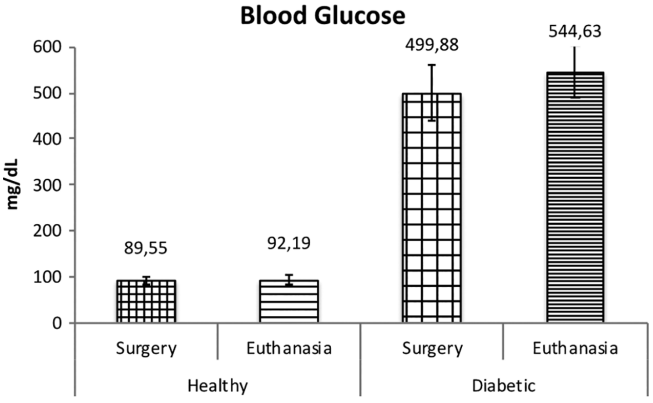

FIGURE 3 Blood glucose (mg/dl) of healthy and diabetic groups at surgery day and before euthanasia

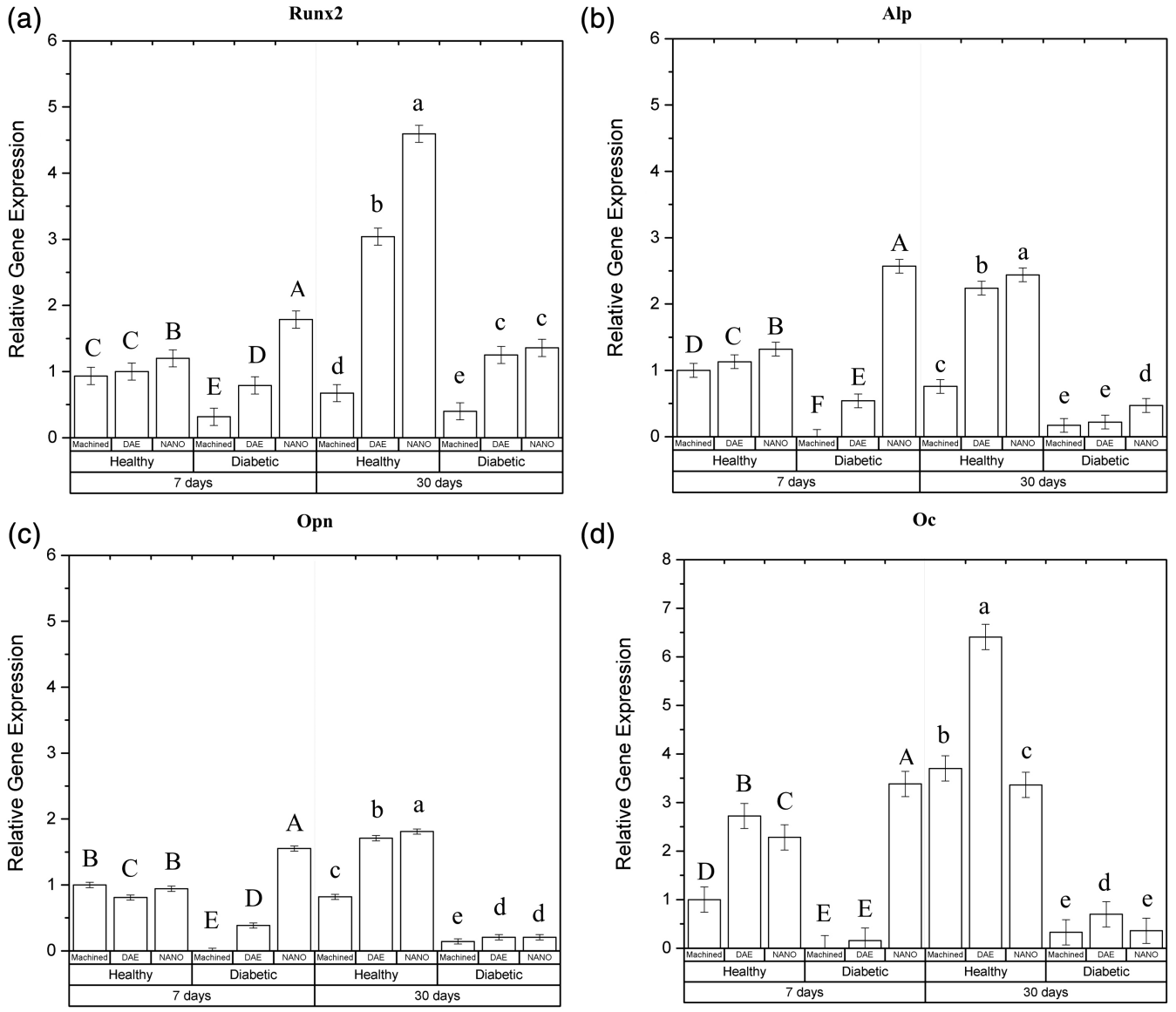

FIGURE 4 (a–d) Relative gene expression of osteogenic markers: Runx2, Alp, Opn and Oc when all factors were collapsed. Identical letters indicate no significant difference among groups

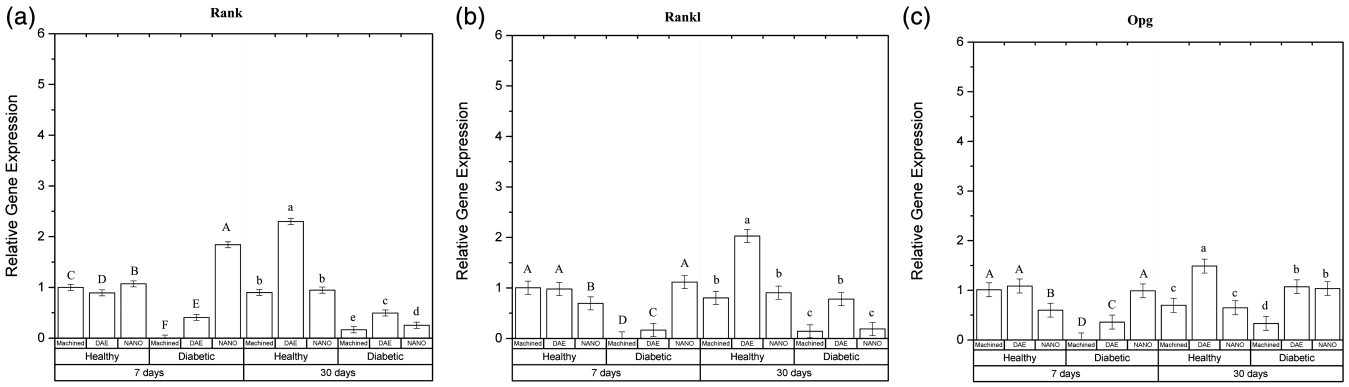

FIGURE 5 (a–c) Relative gene expression of osteogenic markers: Rank, Rankl and Opg when all factors were collapsed. Identical letters indicate no significant difference among groups

30 days. Diabetic NANO 7 days and healthy NANO 30 days presented for Runx2 (Figure 4a)(diabetic NANO 7 days: 1.78 and healthy NANO 30 days: 4.59) ($p < .035$), Alp (Figure 4b) (diabetic NANO 7 days: 2.57 and healthy NANO 30 days: 2.44) ($p < .001$) and Opn (Figure 4c) (diabetic NANO 7 days: 1.55 and healthy NANO 30 days: 0.20) ($p < .001$) statistically significant differences when compared to machined and DAE. Additionally, diabetic NANO 7 days depicted statistically significant differences for Oc (3.38) ($p < .001$) (Figure 4d) and Rank (1.84) ($p < .001$) (Figure 5a) related to other experimental groups. No statistically significant differences were found for Rankl (Figure 5b) and Opg (Figure 5c) however the values of diabetic NANO 7 days were equivalent to healthy DAE 7 days.

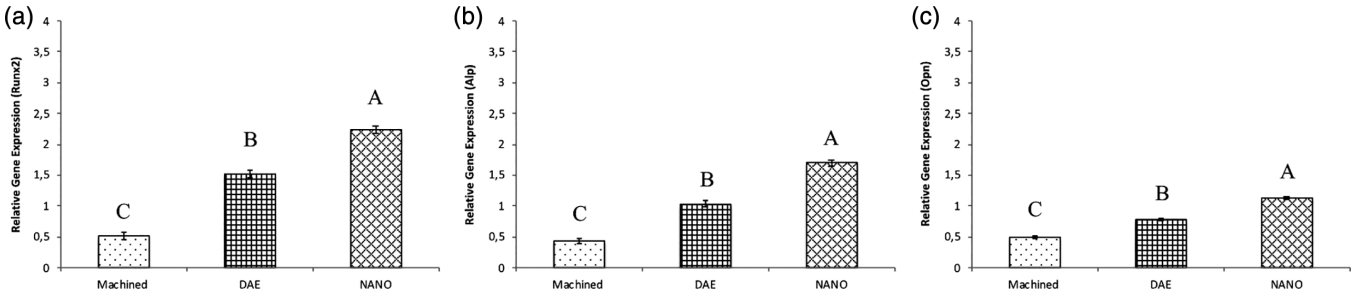

FIGURE 6 (a–c) Runx2, Alp, and Opn as a function of implant surface. Identical letters indicate no significant difference among groups

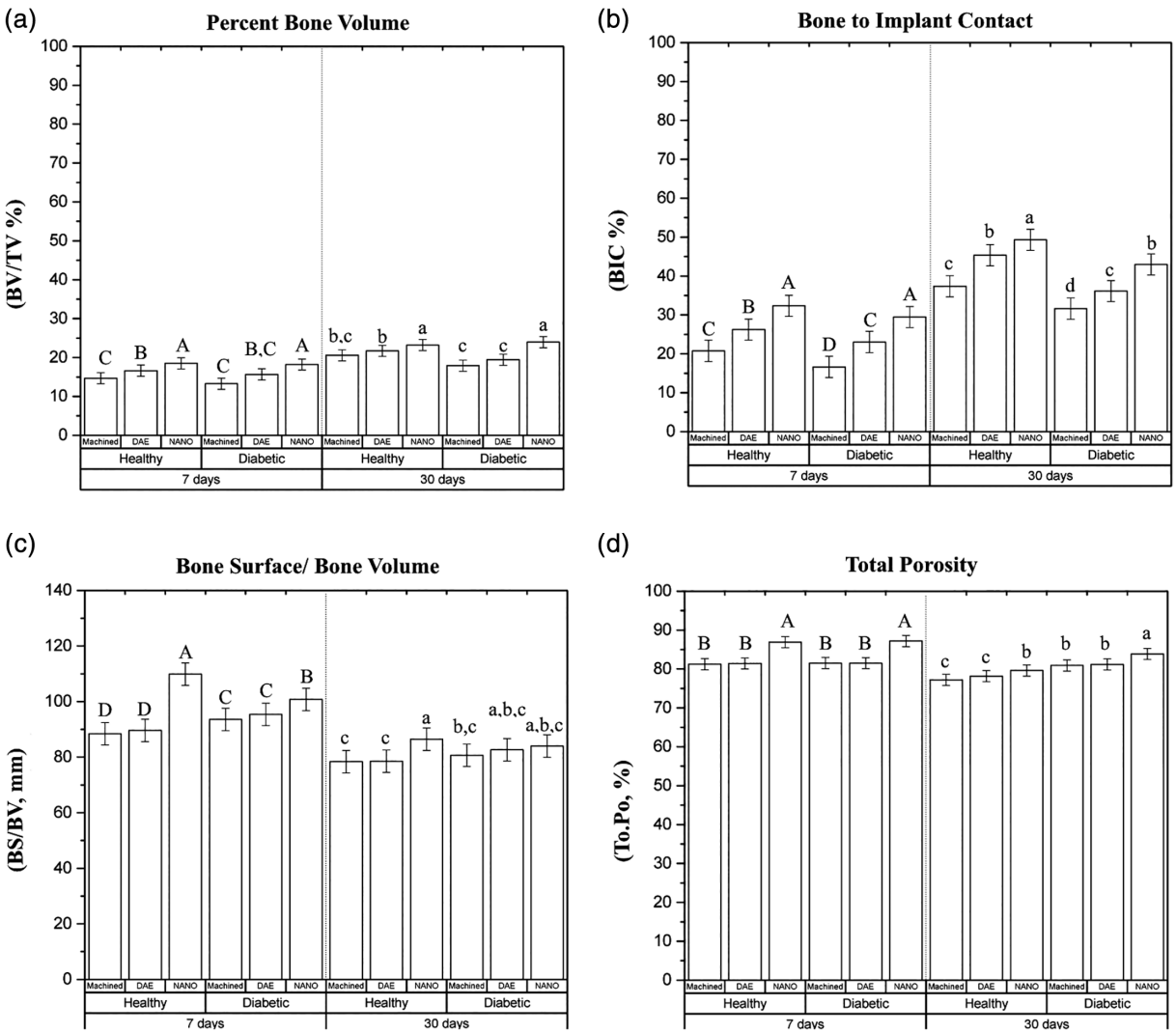

FIGURE 7 (a–d) Microtomographic evaluated parameters (BV/TV, BIC, BS/BV and Po.To) when all factors were collapsed. Identical letters indicate no significant difference among groups

When data were analyzed taking into account the implant surface, Runx2 (NANO: 2.23, DAE: 1.52 and machined: 0.58), Alp (NANO: 1.70, DAE: 1.03 and machined: 0.48), and Opn (NANO: 1.13, DAE: 0.77 and machined: 0.49) showed higher gene expression in NANO group when compared to machined and DAE ($p < .001$) (Figure 6a–c).

The percentage of BV/TV showed statistically significant differences for NANO group irrespective of systemic condition and time point (healthy NANO 7 days: 18,51%, healthy NANO 30 days: 23,20%, diabetic NANO 7 days: 18,20%, and diabetic NANO 30 days: 23,95%) ($p < .001$) (Figure 7a). At 7 days, BIC (healthy: 32,34% and diabetic: 29,47%) ($p < .046$) (Figure 7b), BS/BV (healthy: 109,87 mm) ($p = .003$) (Figure 7c) and Po.To (healthy: 86,90% and diabetic: 83,87%) ($p < .022$) (Figure 7d) depicted statistically significant differences for NANO HA when compared to machined and DAE. At 30 day time point NANO surface revealed statistically significant differences for BIC (healthy: 49,30%) ($p < .046$) and Po.To (diabetic: 83,87%) ($p < .022$) related to machined and DAE (Figure 7b,d).

When data were analyzed taking into account the implant surface, all micro-CT parameters: BV/TV (NANO: 20,97%, DAE: 18,36% and machined: 16,60%), BIC (NANO: 38,52%, DAE: 32,69% and machined: 26,60%), BS/BV (NANO: 95,28 mm, DAE: 86,55 mm and machined: 85,25 mm) and Po.To (NANO: 84,39%, DAE: 80,57% and machined: 80,22%) presented statistically significant differences for NANO surface when compared to machined and DAE ($p < .001$) (Figure 8a–c).

The representative 3D reconstructed images with a focus on the interfacial bone formation on the implants surface in machined, DAE and NANO groups, at 7 and 30 days, and in healthy and diabetic rats is shown in Figure 9. From the image, expressive bone formation can be seen at the implant interface in the NANO group in all time point evaluations and systemic condition.

4 | DISCUSSION

Nowadays, dental implant surgery is one of most successful methods to give back absent teeth. Advances in surface characteristics, design and surgical techniques has made insertion of dental implants a certain and highly successful method, with a mean survival rate of 94.6% and a mean success rate of 89.7% after more than 10 years (Moraschini, Poubel, Ferreira, & Barboza, 2015). In this study, the effects of nanostructured HA coated implant surface (NANO) were observed after 7 and 30 days, in healthy and diabetic animals (as a model of impaired bone healing).

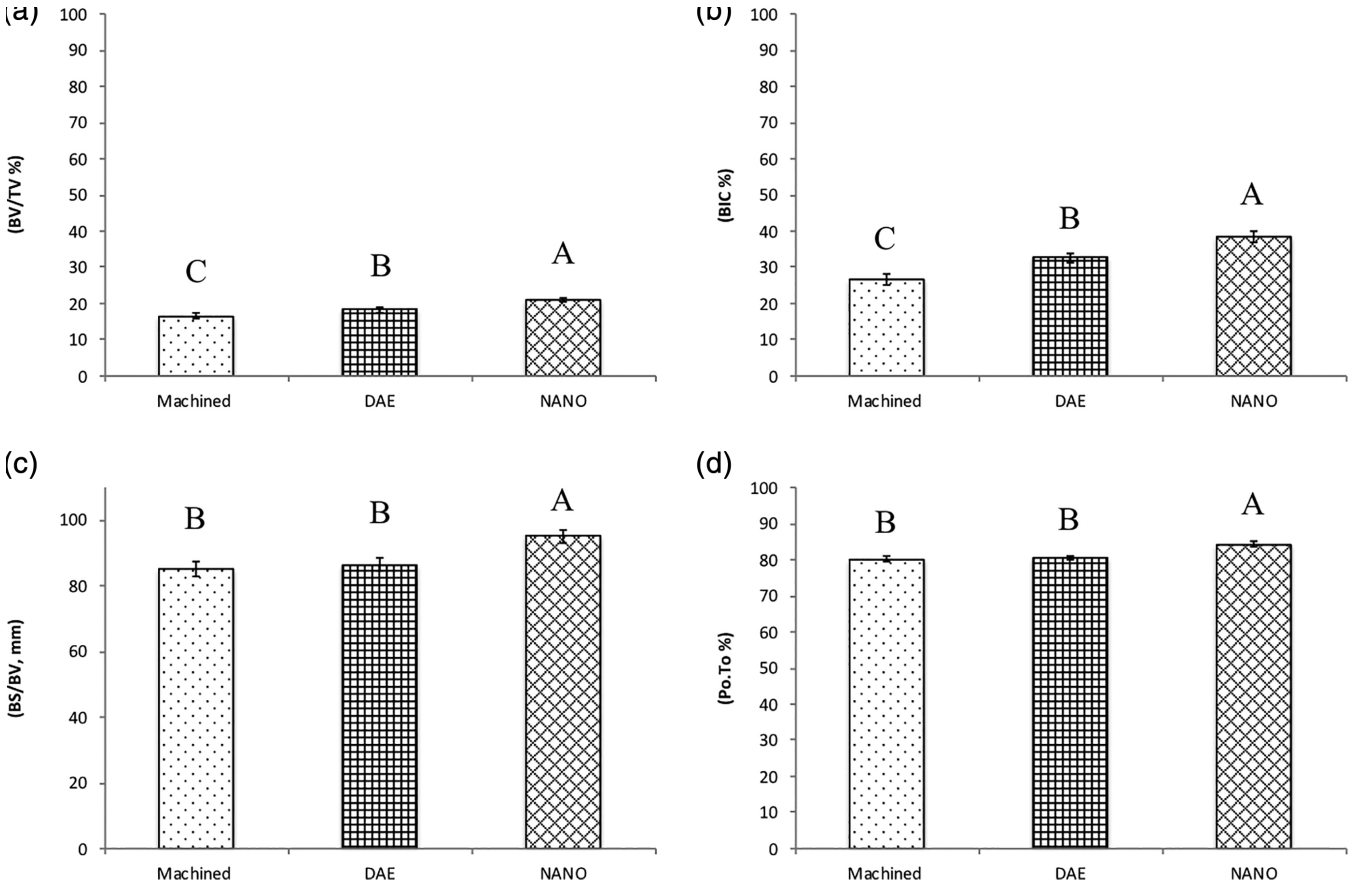

FIGURE 8 (a–c) BV/TV, BIC, BS/BV and Po.To as a function of implant surface. Identical letters indicate no significant difference among groups

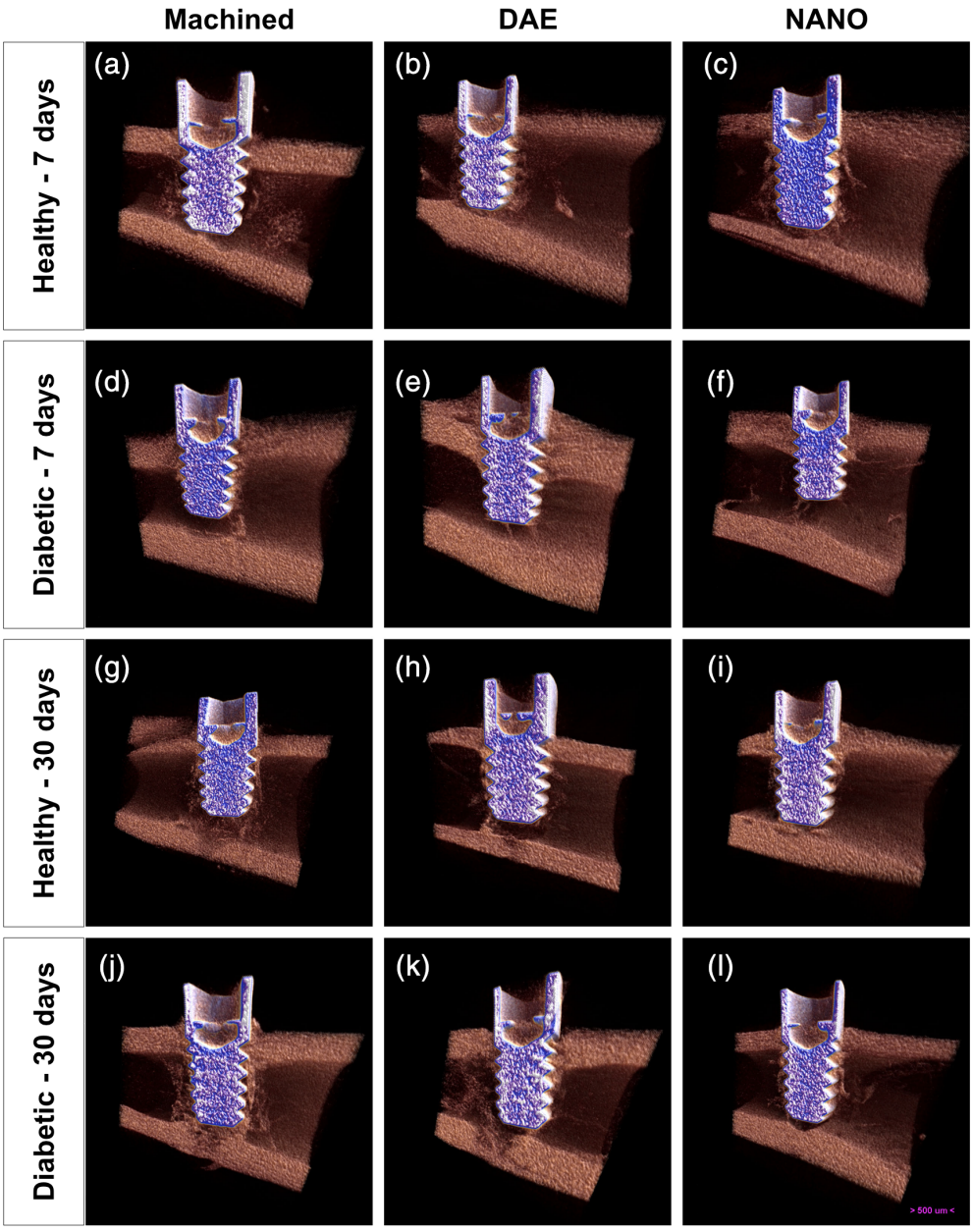

FIGURE 9 The representative 3D reconstructed images with a focus on the interfacial bone formation on implants surface of machined (a, d, g, j), DAE (b, e, h, k) and NANO (c, f, i, l) groups in healthy (a–c and g–i) and diabetic (d–f and j–l) rats at 7 (a–f) and 30 (g–l) days. From the images, significant bone formation can be observed at the implant interface in the NANO group in all time point evaluation and systemic condition

Numerous methods of depositing HA on metallic implants have been reported (Lemons, 1988; de Lange & Donath, 1989; Kay, 1992). The coating methods tend to modify the properties of the starting material as a result of temperature and time at temperature that the HA raw material is exposed to during the deposition of coating (de Groot, Geesink, Klein, & Serekian, 1987; Ong & Lucas, 1994; Ong, Lucas, Lacefield, & Rigney, 1992). These modifications can result in alterations in the basic structure and chemistry of material or changes in the form of coating becoming contaminated by foreign materials (Ducheyne, 1987; Kay, 1988). Additionally, studies have revealed problems related by poor adhesion between the coatings and metallic substrates (Filiaggi, Coombs, & Pilliar, 1991).

Buser et al., (1991) evaluated the influence of different surface characteristics on bone integration of titanium implants and showed that HA plasma-sprayed coating revealed signs of resorption concluding that this particular HA coating is biologically unstable. This state of the calcium phosphate is expected to be less stable and prone to biologic degradation (Buser et al., 1991). These findings confirm observations in other studies where resorption of HA plasma-sprayed coatings was also reported (de Lange & Donath, 1989; Denissen, Kalk, de Nieuport, Maltha, & van de Hooff, 1990). Applying a nanocrystalline thin coating, below 100 nm in thickness, on an implant surface, reduces many of the risks associated with thick plasma sprayed coatings, such as delamination, crack formation and unpredictable resorption. In this study, the NANO surface treatment was performed using a coating liquid containing nanosized hydroxyapatite crystals and placed in an oven at 450°C for 5 min for sintering and stable adhesion of the HA crystals. This method makes it possible to change the chemistry of the surface (i.e., from titanium to HA), while preserving the

micro roughness of the substrate, and also introducing a roughness on the nanometer level.

One of the most important features for enhancement of osseointegration is to balance the relationship between cell proliferation and cell differentiation, simultaneously stimulating both events (Schwartz, Olivares-Navarrete, Wieland, Cochran, & Boyan, 2009). Nanotopography shows an important role in several cellular responses (Curtis & Wilkinson, 1999), since cell/matrix/substrate interactions associated with cell signaling occur at the nanometer level. Such signals regulate migration, proliferation, adhesion, and cell spreading, as well as differentiation and both gene and protein expression (Globus, Moursi, Zimmerman, Lull, & Damsky, 1995; Schneider, Zaharias, & Stanford, 2001). These characteristics influence the biological response to implantable devices by accelerating tissue healing and later osseointegration (Dang et al., 2016; Longo et al., 2016).

It has been shown that nanotopographies have a positive effect on several aspects of osteogenesis (Chen et al., 2017; MSC-R et al., 2016). Lopes et al. (2019a), evaluated the expression of key osteoblastic markers and confirmed the osteogenic potential of nanostructured surface even under nonosteogenic conditions. Martinez et al. (2018) showed that, when osteoblasts were grown into a nanotopography, greater cell spreading, proliferation, and viability, as well as increased expression of two proteins involved in the initial osseointegration process were observed, when compared with a surface treated by double etching alone. Furthermore, other studies depicted the benefits of NANO surface (de Oliveira, Zalzal, Beloti, Rosa, & Nanci, 2007; Jimbo et al., 2011; Longo et al., 2016; Lopes et al., 2019b; Lopes et al., 2020). In the present study, gene expression (Runx2, Alp and Opn) and micro-CT (BV/TV, BIC, BS/BV and Po. To) analysis revealed the superiority of NANO surface when compared to machined and DAE (data as a function of implant surface).

Previous studies showed the importance of DM on implant osseointegration in experimental diabetic models (McCracken, Lemons, Rahemtulla, Prince, & Feldman, 2000; Takeshita et al., 1997). Considerable clinical and experimental evidence indicates that DM patients face much higher rates of implant loosening or failure compared to healthy individuals, due to delayed peri-implant bone formation and suboptimal bone–implant contact (Moraschini, Barboza, & Peixoto, 2016). Moreover, evidence suggests that the cell functions (e.g., cell metabolic activity, mineralization, and multi-directional differentiation) of bone marrow stromal cells are impaired under diabetic conditions (Qian, Zhu, Yu, Jiang, & Zhang, 2015; Rabbani et al., 2019; Shin & Peterson, 2012).

The values found in the present study for healthy (surgery: 89.55 ± 8.88 and euthanasia: 92.19 ± 9.67) and diabetic (surgery: 499.88 ± 62.27 and euthanasia: 544.63 ± 57.07) rats were in agreement with literature (Margonar et al., 2003; McCracken et al., 2000; Nevins, Karimbux, Weber, Giannobile, & Fiorellini, 1998). Margonar et al., 2003 used the same parameter (blood glucose levels at or above 300 mg/dl), and implied that more elevated blood glucose concentrations could lead to more severe modifications on bone biology (Margonar et al., 2003). The new bone formed around implants was described like young and disorganized in diabetic animals when compared to the non-diabetic controls, recommending important distinctions in this new bone (Nevins et al., 1998).

Bone formation is a complex metabolic process that includes the functional activities of osteoblasts and osteoclasts along with the interactions between these cells, thereby contributing to a balance between bone formation and resorption (Sivaraj & Adams, 2016). Increasing evidence suggests that DM not only interferes with bone formation by decreasing the expression of osteoblastogenes is related factors, it also elevates bone resorption and loss via abnormally high mitochondrial reactive oxygen species levels, which lead to RANKL-mediated osteoclast activation and differentiation (Hamann et al., 2011; Napoli et al., 2017). Ramenzoni et al., 2020 revealed the clinical implications that high glucose levels combined with inflammation can induce, decreasing osteoblast processes, including the proliferation and differentiation (Ramenzoni, Bosch, Proksch, Attin, & Schmidlin, 2020).

In the present study, RankL and Opg presented the same gene expression profile. There was no statistical significant difference regarding implant surface. However, when data was evaluated in a function of systemic condition, the results of Opg in NANO group (diabetic 7 days: 0,99) presented comparable values to healthy groups of the other surfaces (machined 7 days: 1,01 and DAE 7 days: 1,08), suggesting a similar bone remodeling mechanism.

Opn is an important protein in the formation of noncollagenous bone matrix and is expressed by various cell types, including osteoclasts and osteoblasts (Wai & Kuo, 2008). Its also regulates angiogenesis as a response to cell stress, cell adhesion, chemotaxis, and cell motility (Wai & Kuo, 2004). Martinez et al. (2018) in a in vitro study, demonstrated osteoblasts seeded onto the surface treated with HA nanocrystals presented higher expression of type I collagen and Opn, when compared with the DAE surface, especially after 72 and 24 hr.

In this animal work, some findings indicated that the NANO-HA surface may be less affected by these adverse effects of the high glucose environment: the levels of Runx2 (DN7d: 1.78), Alp (DN7d: 2.57), Opn (DN7d: 1.55), and Oc (DN7d: 3.38) suggests an enhancement of osteoblast proliferation, mainly at early stages of osseointegration. Additionally, literature findings support the evidence through previous animal studies that demonstrated NANO complex surfaces outperforming microtopography surfaces in metabolically compromised subjects (Ajami et al., 2014; Ajami, Bell, Liddell, & Davies, 2016; Schlegel et al., 2013).

3D appraisal with micro-CT has been widely used nowadays due to the fact that it makes it easier to examine and quantify the bone formation around implants or bone substitutes in a 3D plane (Sarve, Lindblad, Borgefors, & Johansson, 2011). High-resolution 3D imaging techniques, such as micro-CT, directly measure bone microarchitecture. This study evaluated by micro-CT analysis the percent bone volume (BV/TV, %), percent intersection surface (IS/TS, %), bone surface/volume ratio (BS/BV, mm), and total porosity (To.Po, %).

Zhou et al. (2019) evaluated if surface modifications can improve osseointegration in a setting with DM and revealed that the amount of newly formed bone in the 200-mm-wide zone parallel to the implant contour was increased in the sandblasted and acid etched

group (SLA) (16.9%) and the HA coated surface group (14.9%) compared with the machined group (11.4%) . However, only the difference between the SLA group and the machined group was statistically significant. In the present study, the percentage of IS/TS results showed that the NANO HA coating presented statistically significant difference when compared to machined and DAE surfaces, irrespective of time and systemic condition. This evidence can suggest that the new implant surface could compensate the limitations of an impaired bone-healing model. The findings of this work were in concordance with other studies that demonstrate that nanoscale modified titanium surfaces curbs the effect of high glucose concentrations (Ajami et al., 2014; Ajami et al., 2016; Ma et al., 2017). Additionally, the micro/nano-structured titanium surface has an advantageous effect on osteoblast proliferation and differentiation in diabetic serum (Jiang et al., 2017).

The micro-CT analysis of BV/TV (%), BS/BV (mm) and Po.To (%) showed higher values, better arranged bone shapes and higher volume densities for NANO group in all evaluated time point and irrespective of systemic condition compared to other experimental groups, but BS/BV (30 days healthy group and 7 and 30 days diabetic group), implying a better bone reaction in these groups. Our findings are in accordance with Ajami and collaborators that performed a microtomographic and histologic study using euglycemic and hyperglycemic rats and conclude that poor implant osseointegration in hyperglycemia is counteracted by the addition of nanotopographical attributes to a microtopographically complex implant surface (Ajami et al., 2014). Controversially, Zhou et al., in 2019, exhibited no significant differences in BV/TV between the machined, sandblasted and acid etched, and HA coated surface groups, in a diabetic rat model (Zhou et al., 2019).

The amount of bone surrounding implants surface differed across different implant treatments, systemic condition and time. Bone development at the implant interface was higher (i.e., direct bone contact to the implant) in NANO groups irrespective of systemic condition and time. Together with image reconstruction, it was simple to find the condition of cancellous bone genesis to the implant surface, which gives supplementary knowledge from both qualitative and quantitative outlooks.

5 | CONCLUSION

Microtomographic and gene expression analyses have shown the benefits of nano-hydroxyapatite coating implants in promoting new bone formation in diabetic animals when compared to machined and double acid etched surfaces. Thus, this surface may represent a promising alternative for replacing missing teeth in compromised subjects. Clinical studies are needed to better confirm this effect in humans.

ACKNOWLEDGMENTS

Fabíola Singaretti de Oliveira, Adriana Luisa Gonçalves de Almeida, Milla Sprone Tavares and Roger Rodrigo Fernandes are thankful for their technical attendance along the laboratory essays.

ORCID

Sérgio Luís Scombatti de Souza https://orcid.org/0000-0002-6199-7348

REFERENCES

Ajami, E., Bell, S., Liddell, R. S., & Davies, J. E. (2016). Early bone anchorage to micro- and nano-topographically complex implant surfaces in hyperglycemia. *Acta Biomaterialia*, *39*, 169–179.

Ajami, E., Mahno, E., Mendes, V. C., Bell, S., Moineddin, R., & Davies, J. E. (2014). Bone healing and the effect of implant surface topography on osteoconduction in hyperglycemia. *Acta Biomaterialia*, *10*(1), 394–405.

Albrektsson, T., Branemark, P. I., Hansson, H. A., & Lindstrom, J. (1981). Osseointegrated titanium implants. Requirements for ensuring a long-lasting, direct bone-to-implant anchorage in man. *Acta Orthopaedica Scandinavica*, *52*(2), 155–170.

Buser, D., Schenk, R. K., Steinemann, S., Fiorellini, J. P., Fox, C. H., & Stich, H. (1991). Influence of surface characteristics on bone integration of titanium implants. A histomorphometric study in miniature pigs. *Journal of Biomedical Materials Research*, *25*(7), 889–902.

Chen, Z., Bachhuka, A., Wei, F., Wang, X., Liu, G., Vasilev, K., & Xiao, Y. (2017). Nanotopography-based strategy for the precise manipulation of osteoimmunomodulation in bone regeneration. *Nanoscale*, *9*(46), 18129–18152.

Chuang, S. K., Tian, L., Wei, L. J., & Dodson, T. B. (2001). Kaplan-Meier analysis of dental implant survival: A strategy for estimating survival with clustered observations. *Journal of Dental Research*, *80*(11), 2016–2020.

Coelho, P. G., Granjeiro, J. M., Romanos, G. E., Suzuki, M., Silva, N. R., Cardaropoli, G., … Lemons, J. E. (2009). Basic research methods and current trends of dental implant surfaces. *Journal of Biomedical Materials Research. Part B, Applied Biomaterials*, *88*(2), 579–596.

Courtney, M. W., Jr., Snider, T. N., & Cottrell, D. A. (2010). Dental implant placement in type II diabetics: A review of the literature. *Journal of the Massachusetts Dental Society*, *59*(1), 12–14.

Curtis, A., & Wilkinson, C. (1999). New depths in cell behaviour: Reactions of cells to nanotopography. *Biochemical Society Symposium*, *65*, 15–26.

Dang, Y., Zhang, L., Song, W., Chang, B., Han, T., Zhang, Y., & Zhao, L. (2016). In vivo osseointegration of Ti implants with a strontium-containing nanotubular coating. *International Journal of Nanomedicine*, *11*, 1003–1011.

de Groot, K., Geesink, R., Klein, C. P., & Serekian, P. (1987). Plasma sprayed coatings of hydroxylapatite. *Journal of Biomedical Materials Research*, *21*(12), 1375–1381.

de Lange, G. L., & Donath, K. (1989). Interface between bone tissue and implants of solid hydroxyapatite or hydroxyapatite-coated titanium implants. *Biomaterials*, *10*(2), 121–125.

de Oliveira, P. T., Zalzal, S. F., Beloti, M. M., Rosa, A. L., & Nanci, A. (2007). Enhancement of in vitro osteogenesis on titanium by chemically produced nanotopography. *Journal of Biomedical Materials Research. Part A*, *80*(3), 554–564.

Denissen, H. W., Kalk, W., de Nieuport, H. M., Maltha, J. C., & van de Hooff, A. (1990). Mandibular bone response to plasma-sprayed coatings of hydroxyapatite. *The International Journal of Prosthodontics*, *3*(1), 53–58.

Ducheyne, P. (1987). Bioceramics: Material characteristics versus in vivo behavior. *Journal of Biomedical Materials Research*, *21*(A2 Suppl), 219–236.

Expert Committee on the Diagnosis and Classification of Diabetes Mellitus. (2003). Report of the expert committee on the diagnosis and classification of diabetes mellitus. *Diabetes Care*, *23*(Suppl 1), S5–S20.

Feldkamp, L. A., Goldstein, S. A., Parfitt, A. M., Jesion, G., & Kleerekoper, M. (1989). The direct examination of three-dimensional bone architecture in vitro by computed tomography. *Journal of Bone and Mineral Research*, *4*(1), 3–11.

Filiaggi, M. J., Coombs, N. A., & Pilliar, R. M. (1991). Characterization of the interface in the plasma-sprayed HA coating/Ti-6Al-4V implant system. *Journal of Biomedical Materials Research*, *25*(10), 1211–1229.

Gittens, R. A., McLachlan, T., Olivares-Navarrete, R., Cai, Y., Berner, S., Tannenbaum, R., … Boyan, B. D. (2011). The effects of combined micron–/submicron-scale surface roughness and nanoscale features on cell proliferation and differentiation. *Biomaterials*, *32*(13), 3395–3403.

Globus, R. K., Moursi, A., Zimmerman, D., Lull, J., & Damsky, C. (1995). Integrin-extracellular matrix interactions in connective tissue remodeling and osteoblast differentiation. *ASGSB Bulletin*, *8*(2), 19–28.

Goodman, W. G., & Hori, M. T. (1984). Diminished bone formation in experimental diabetes. Relationship to osteoid maturation and mineralization. *Diabetes*, *33*(9), 825–831.

Hamann, C., Goettsch, C., Mettelsiefen, J., Henkenjohann, V., Rauner, M., Hempel, U., … Rammelt, S. (2011). Others. Delayed bone regeneration and low bone mass in a rat model of insulin-resistant type 2 diabetes mellitus is due to impaired osteoblast function. *American Journal of Physiology. Endocrinology and Metabolism*, *301*(6), E1220–E1228.

Jiang, H., Ma, X., Zhou, W., Dong, K., Rausch-Fan, X., Liu, S., & Li, S. (2017). The effects of hierarchical micro/Nano-structured titanium surface on osteoblast proliferation and differentiation under diabetic conditions. *Implant Dentistry*, *26*(2), 263–269.

Jimbo, R., Coelho, P. G., Vandeweghe, S., Schwartz-Filho, H. O., Hayashi, M., Ono, D., … Wennerberg, A. (2011). Histological and three-dimensional evaluation of osseointegration to nanostructured calcium phosphate-coated implants. *Acta Biomaterialia*, *7*(12), 4229–4234.

Kay, J. F. (1988). Designing to counteract the effects of initial device instability: Materials and engineering. *Journal of Biomedical Materials Research*, *22*(12), 1127–1136.

Kay, J. F. (1992). Calcium phosphate coatings for dental implants. Current status and future potential. *Dental Clinics of North America*, *36*(1), 1–18.

Kjellin P, Andersson M; *Synthetic Nano-sized crystalline calcium phosphate and method of production. Patent US patent 8206813*. 2012.Alexandria, VA, USA: US Patent and Trademark Office.

Lemons, J. E. (1988). Hydroxyapatite coatings. *Clinical Orthopaedics and Related Research*, *235*, 220–223.

Li, Z., Kuhn, G., von Salis-Soglio, M., Cooke, S. J., Schirmer, M., Muller, R., & Ruffoni, D. (2015). In vivo monitoring of bone architecture and remodeling after implant insertion: The different responses of cortical and trabecular bone. *Bone*, *81*, 468–477.

Livak, K. J., & Schmittgen, T. D. (2001). Analysis of relative gene expression data using real-time quantitative PCR and the 2(−Delta Delta C[T]) method. *Methods*, *25*(4), 402–408.

Longo, G., Ioannidu, C. A., Scotto d'Abusco, A., Superti, F., Misiano, C., Zanoni, R., … Scandurra, F. (2016). Improving osteoblast response in vitro by a nanostructured thin film with titanium carbide and titanium oxides clustered around graphitic carbon. *PLoS One*, *11*(3), e0152566.

Lopes, H. B., Freitas, G. P., Elias, C. N., Tye, C., Stein, J. L., Stein, G. S., … Beloti, M. M. (2019b). Participation of integrin beta3 in osteoblast differentiation induced by titanium with nano or microtopography. *Journal of Biomedical Materials Research. Part A*, *107*(6), 1303–1313.

Lopes, H. B., Freitas, G. P., Fantacini, D. M. C., Picanco-Castro, V., Covas, D. T., Rosa, A. L., & Beloti, M. M. (2019a). Titanium with nanotopography induces osteoblast differentiation through regulation of integrin alphaV. *Journal of Cellular Biochemistry*, *120*(10), 16723–16732.

Lopes, H. B., Souza, A. T. P., Freitas, G. P., Elias, C. N., Rosa, A. L., & Beloti, M. M. (2020). Effect of focal adhesion kinase inhibition on osteoblastic cells grown on titanium with different topographies. *Journal of Applied Oral Science*, *28*, e20190156.

Ma, X. Y., Feng, Y. F., Wang, T. S., Lei, W., Li, X., Zhou, D. P., … Wang, L. (2017). Involvement of FAK-mediated BMP-2/Smad pathway in mediating osteoblast adhesion and differentiation on nano-HA/chitosan composite coated titanium implant under diabetic conditions. *Biomaterials Science*, *6*(1), 225–238.

Margonar, R., Sakakura, C. E., Holzhausen, M., Pepato, M. T., Alba j, R., & Marcantonio j, E. (2003). The influence of diabetes mellitus and insulin therapy on biomechanical retention around dental implants: A study in rabbits. *Implant Dentistry*, *12*(4), 333–339.

Martinez, E. F., Ishikawa, G. J., de Lemos, A. B., Barbosa Bezerra, F. J., Sperandio, M., & Napimoga, M. H. (2018). Evaluation of a titanium surface treated with hydroxyapatite nanocrystals on osteoblastic cell behavior: An in vitro study. *The International Journal of Oral & Maxillofacial Implants*, *33*(3), 597–602.

McCracken, M., Lemons, J. E., Rahemtulla, F., Prince, C. W., & Feldman, D. (2000). Bone response to titanium alloy implants placed in diabetic rats. *The International Journal of Oral & Maxillofacial Implants*, *15*(3), 345–354.

Meirelles, L., Arvidsson, A., Albrektsson, T., & Wennerberg, A. (2007). Increased bone formation to unstable nano rough titanium implants. *Clinical Oral Implants Research*, *18*(3), 326–332.

Moraschini, V., Barboza, E. S., & Peixoto, G. A. (2016). The impact of diabetes on dental implant failure: A systematic review and meta-analysis. *International Journal of Oral and Maxillofacial Surgery*, *45*(10), 1237–1245.

Moraschini, V., Poubel, L. A., Ferreira, V. F., & Barboza, E. S. (2015). Evaluation of survival and success rates of dental implants reported in longitudinal studies with a follow-up period of at least 10 years: A systematic review. *International Journal of Oral and Maxillofacial Surgery*, *44*(3), 377–388.

MSC-R, L., M, S. F., L, N. T., E, P. F., H, B. L., TdO, P., … Beloti, M. M. (2016). Titanium with Nanotopography induces osteoblast differentiation by regulating endogenous Bone morphogenetic protein expression and signaling pathway. *Journal of Cellular Biochemistry*, *117*(7), 1718–1726.

Napoli, N., Chandran, M., Pierroz, D. D., Abrahamsen, B., Schwartz, A. V., Ferrari, S. L., … Diabetes Working, G. (2017). Mechanisms of diabetes mellitus-induced bone fragility. *Nature Reviews. Endocrinology*, *13*(4), 208–219.

Nevins, M. L., Karimbux, N. Y., Weber, H. P., Giannobile, W. V., & Fiorellini, J. P. (1998). Wound healing around endosseous implants in experimental diabetes. *The International Journal of Oral & Maxillofacial Implants*, *13*(5), 620–629.

Odgaard, A. (1997). Three-dimensional methods for quantification of cancellous bone architecture. *Bone*, *20*(4), 315–328.

Ong, J. L., & Lucas, L. C. (1994). Post-deposition heat treatments for ion beam sputter deposited calcium phosphate coatings. *Biomaterials*, *15*(5), 337–341.

Ong, J. L., Lucas, L. C., Lacefield, W. R., & Rigney, E. D. (1992). Structure, solubility and bond strength of thin calcium phosphate coatings produced by ion beam sputter deposition. *Biomaterials*, *13*(4), 249–254.

Qian, C., Zhu, C., Yu, W., Jiang, X., & Zhang, F. (2015). High-fat diet/low-dose Streptozotocin-induced type 2 Diabetes in rats impacts osteogenesis and Wnt signaling in Bone marrow stromal cells. *PLoS One*, *10*(8), e0136390.

Rabbani, P. S., Soares, M. A., Hameedi, S. G., Kadle, R. L., Mubasher, A., Kowzun, M., & Ceradini, D. J. (2019). Dysregulation of Nrf2/Keap1 redox pathway in Diabetes affects multipotency of stromal cells. *Diabetes*, *68*(1), 141–155.

Ramenzoni, L. L., Bosch, A., Proksch, S., Attin, T., & Schmidlin, P. R. (2020). Effect of high glucose levels and lipopolysaccharides-induced inflammation on osteoblast mineralization over sandblasted/acid-etched titanium surface. *Clinical Implant Dentistry and Related Research*, *22*(2), 213–219.

Retzepi, M., & Donos, N. (2010). The effect of diabetes mellitus on osseous healing. *Clinical Oral Implants Research*, *21*(7), 673–681.

Sarve, H., Lindblad, J., Borgefors, G., & Johansson, C. B. (2011). Extracting 3D information on bone remodeling in the proximity of titanium

implants in SRmuCT image volumes. *Computer Methods and Programs in Biomedicine*, *102*(1), 25–34.

Schlegel, K. A., Prechtl, C., Most, T., Seidl, C., Lutz, R., & von Wilmowsky, C. (2013). Osseointegration of SLActive implants in diabetic pigs. *Clinical Oral Implants Research*, *24*(2), 128–134.

Schneider, G. B., Zaharias, R., & Stanford, C. (2001). Osteoblast integrin adhesion and signaling regulate mineralization. *Journal of Dental Research*, *80*(6), 1540–1544.

Schwartz, Z., Olivares-Navarrete, R., Wieland, M., Cochran, D. L., & Boyan, B. D. (2009). Mechanisms regulating increased production of osteoprotegerin by osteoblasts cultured on microstructured titanium surfaces. *Biomaterials*, *30*(20), 3390–3396.

Shin, L., & Peterson, D. A. (2012). Impaired therapeutic capacity of autologous stem cells in a model of type 2 diabetes. *Stem Cells Translational Medicine*, *1*(2), 125–135.

Sivaraj, K. K., & Adams, R. H. (2016). Blood vessel formation and function in bone. *Development*, *143*(15), 2706–2715.

Souza, A. T. P., Bezerra, B. L. S., Oliveira, F. S., Freitas, G. P., Bighetti Trevisan, R. L., Oliveira, P. T., … Beloti, M. M. (2018). Effect of bone morphogenetic protein 9 on osteoblast differentiation of cells grown on titanium with nanotopography. *Journal of Cellular Biochemistry*, *119*, 8441–8449.

Takeshita, F., Iyama, S., Ayukawa, Y., Kido, M. A., Murai, K., & Suetsugu, T. (1997). The effects of diabetes on the interface between hydroxyapatite implants and bone in rat tibia. *Journal of Periodontology*, *68*(2), 180–185.

Vandeweghe, S., Coelho, P. G., Vanhove, C., Wennerberg, A., & Jimbo, R. (2013). Utilizing micro-computed tomography to evaluate bone structure surrounding dental implants: A comparison with histomorphometry. *Journal of Biomedical Materials Research. Part B, Applied Biomaterials*, *101*(7), 1259–1266.

Wai, P. Y., & Kuo, P. C. (2004). The role of Osteopontin in tumor metastasis. *The Journal of Surgical Research*, *121*(2), 228–241.

Wai, P. Y., & Kuo, P. C. (2008). Osteopontin: Regulation in tumor metastasis. *Cancer Metastasis Reviews*, *27*(1), 103–118.

Zhou, W., Tangl, S., Reich, K. M., Kirchweger, F., Liu, Z., Zechner, W., … Rausch-Fan, X. (2019). The influence of type 2 Diabetes mellitus on the Osseointegration of titanium implants with different surface modifications-a Histomorphometric study in high-fat diet/low-dose Streptozotocin-treated rats. *Implant Dentistry*, *28*(1), 11–19.

How to cite this article: de Oliveira PGFP, de Melo Soares MS, Silveira e Souza AMM, et al. Influence of nanohydroxyapatite coating implants on gene expression of osteogenic markers and micro-CT parameters. An in vivo study in diabetic rats. *J Biomed Mater Res*. 2021;109:682–694. https://doi.org/10.1002/jbm.a.37052